# Wave Propagation and Damage Localization in Thick-Walled Hollow Cylinders Through Inner Sensing

YUANMAN ZHANG[1], SHENGBO SHAN[2] and LI CHENG[3]

## ABSTRACT

Thick-walled hollow cylinders (TWHCs) are widely used in engineering structures and transportation systems, exemplified by train axles. The real-time and online health monitoring of such structures is crucial to ensure their structural integrity and operational safety. While elastic-wave-based structural health monitoring (SHM) shows promise, the development of feasible methods strongly relies on a good understanding and exploitation of the wave propagation properties and their interaction with structural defects. TWHCs usually bear multiple wave modes, which is a less investigated and explored topic as compared with thin-walled structures. This work examines this issue and proposes a dedicated damage localization strategy by using the selected waves captured on the inner surface of a TWHC. It is shown that, alongside the quasi-surface waves on the outer surface, longitudinal waves converted from the thickness-through shear bulk waves are generated to propagate along the inner surface. Their propagation characteristics are exploited for damage localization based on hyperbolic loci methods through inner surface sensing. Numerical studies are conducted to validate the method, alongside experimental verifications on a benchmark TWHC containing a notch-type defect. Studies provide guidance on damage detection in TWHCs and sensor network design.

## INTRODUCTION

Thick-walled hollow cylindrical structures (TWHCs) are widely used as major structural components in mechanical systems, exemplified by train axles[1]. During service, structural damages, such as cracks and corrosions etc., might initiate and evolve, which jeopardizes the safe operation of the system or even leads to catastrophic failure. Therefore, real-time and online monitoring of such structures is crucial. Among existing techniques, structural health monitoring (SHM) based on ultrasonic guided waves shows great promise due to their appealing features such as high sensitivity to damage, low energy consumption and so on[2].

Successful wave-based SHM technique would rely on a thorough understanding of the wave propagation in a given structure and its interaction with structural defects. Analytical solutions on elastic wave propagation in an infinitely long and hollow cylinder were first developed in the late 50s[3], including the propagation of longitudinal[4], torsional[5] and flexural wave modes in the axial direction. Although the proposed theoretical framework is applicable to both thin- and thick-walled hollow cylinders, subsequent studies mainly focused on the former due to the easier generation of pure guided wave modes and their relatively simple propagation pattern. More examples on guided wave as well as their application for the inspection of thin-walled pipes can be found in some comprehensive review papers[5].

[1]Department of Mechanical Engineering, The Hong Kong Polytechnic University, Kowloon, Hong Kong
[2]Hong Kong Branch of National Rail Transit Electrification and Automation Engineering Technology Research Center, The Hong Kong Polytechnic University, Kowloon, Hong Kong
[3]School of Aerospace Engineering and Applied Mechanics, Tongji University, Shanghai 200092, China

When quasi-surface waves encounter a defect during their propagation, wave reflection and scattering occur, a phenomenon that can be used to detect defects in TWHCs. The lack of successful damage localization methods for TWHCs is mainly due to 1) lack of deep and thorough understanding of the propagation characteristics of different mode types inside a typical TWHC; and 2) insufficient effort in the exploration and synthetization of their respective features for damage localization. This forms the main motivation behind the present study.

## WAVE PROPAGATION IN A THICK-WALLED HOLLOW CYLINDER

To examine the elastic wave generation and propagation, finite element models are built for a TWHC with a surface excitation. Two-dimensional models, shown in Fig. 1, are built to represent the two different cross-sections of the TWHC, with nominal material parameters of aluminum, i.e. Young's modulus 71 GPa, mass density 2700 kg/m3 and Poisson's ratio 0.33. To mimic the surface excitation, a point-force, parallel to the top surface of the TWHC, is applied. The excitation signal is a 5-cycle tone burst signal windowed by the Hann function at a central frequency of 300 kHz. To ensure the convergence and the accuracy of the simulation, the largest size of the mesh is set to 1 mm which ensures more than 10 elements per smallest wavelength under consideration. The sampling frequency is set to 10 MHz.

The resultant wavefields are obtained and displayed in Fig. 2, in terms of displacement magnitude. For the first case in Fig. 2(b) (cross-section along longitudinal direction), typical wave packets are identified according to their propagating velocities and wavelengths. Specifically, strong waves propagating along the outer surface of the structure are referred to as quasi-surface waves whose propagating velocity is very close to idealized surface waves. Interestingly, upon reaching the bottom surface, longitudinal waves appear along the inner surface rather than quasi-surface waves.

To better visualize the wave propagation characteristics, different wave components propagating along different paths inside the structure are plotted in Fig. 3 in terms of their respective displacement components in the $z$ direction, whose magnitudes are indicated by color. Along Path A on the upper/outer surface as shown in Fig. 3(a), two different waves can clearly be observed. Strong energy dissipation occurs at the first wave packet which is therefore identified as evanescent wave. The second wave propagates without obvious attenuation at a constant phase velocity at around 2800 m/s, which is deduced from the slope of the wave trajectory. Two paths are selected along the thickness direction as Paths B and D. The wave propagation in the vertical thickness direction (Path B), identified as shear wave, is displayed in Fig. 3(b) in terms of the displacement in the $z$ direction. The path D has an inclined angle of around 45°. The wave with a strong $x$ direction displacement is identified as longitudinal wave, as shown in Fig. 3(d). After the bulk waves reach the bottom/inner surface, mode conversion occurs, thus producing two propagating waves that are clearly observed as shown by the $z$ direction displacement field map along Path C in Fig. 3(c). Through calculating their phase velocities and the time-of-flight, they are further identified as longitudinal waves respectively. The wave propagation along Path E is illustrated in Fig. 3(e). , which shows high similarity with that in Fig. 3(a) with pronounced quasi-surface wave characteristics.

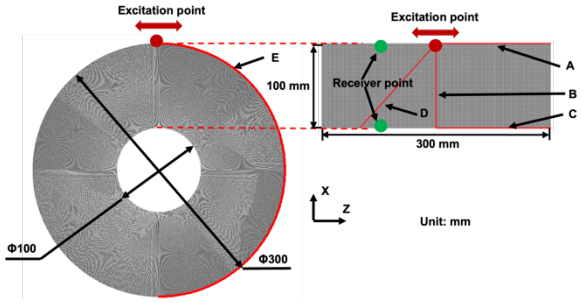


(a) (b)

Figure 1. Cylinder cross-section from (a) radial direction, (b) longitudinal direction.

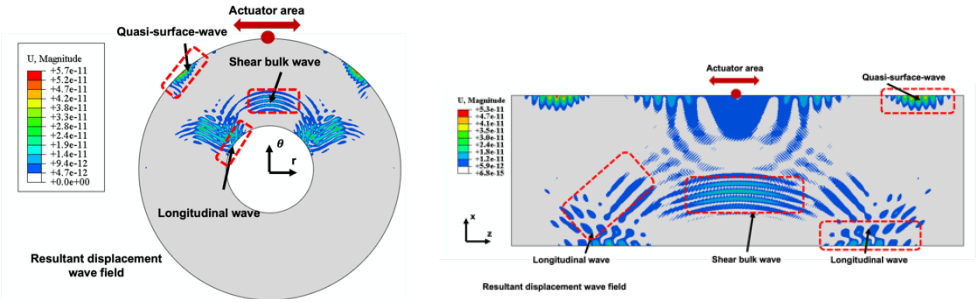


(a) (b)

Figure 2. FE simulated displacement contours of wave propagation. (a) Wave propagation over the cross-section along radial direction, (b) Wave propagation over the cross-section along longitudinal direction.

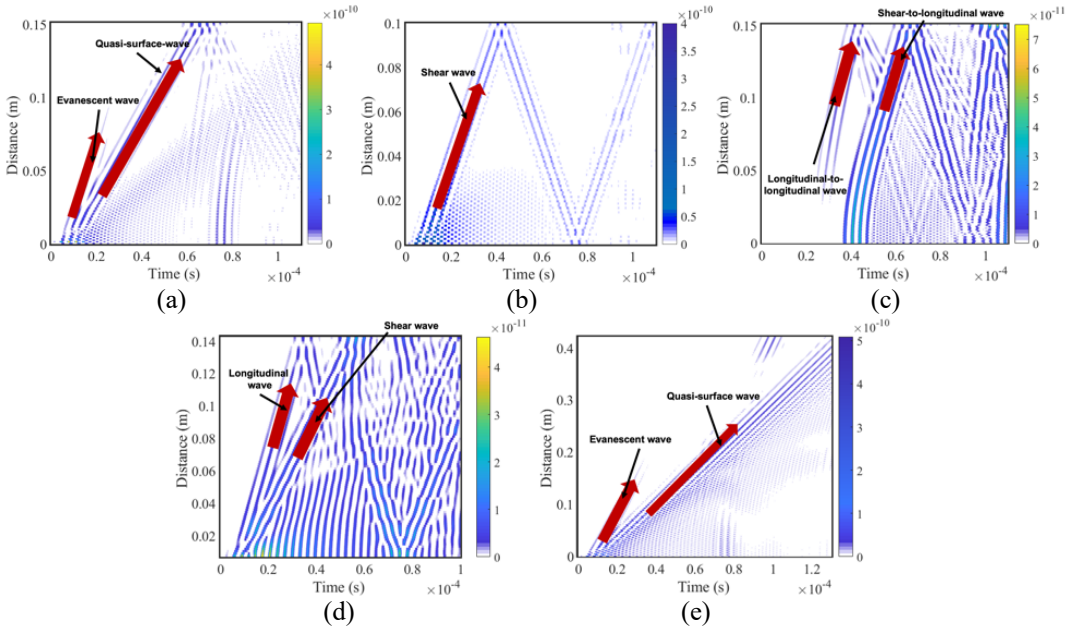


(a) (b) (c)

(d) (e)

Figure 3. FE simulated wave propagation trajectory on (a) Path A, (b) Path B, and (c) Path C, (d) Path D, (e) Path E.

## DAMAGE LOCALIZATION STRATEGY

As illustrated in Fig. 4, two sets of transducer arrays are proposed to be installed on the outer and inner surfaces of a TWHC, respectively. While the former is used as the actuators on the outer surface, the deployment of the latter is to accommodate the need for more practical installation of the transducers.

In light of the revealed mode conversion behavior at the inner surface, the hyperbolic loci method, often used for impact localization, is modified and applied with the sensor array on the inner surface of the TWHC. In this method, the transducers on the outer surface are still used for wave excitation.

For an arbitrary sensor pair s1$(x_{s1}, y_{s1})$-s2$(x_{s2}, y_{s2})$, the time difference of the damage-induced longitudinal waves can be obtained which is further related to the difference distance $D_{d\text{-}c}$ from the damage to the two sensors as

$$D_{d-c} = \left|\sqrt{(x_d - x_{s1})^2 + (y_d - y_{s1})^2} - \sqrt{(x_d - x_{s2})^2 + (y_d - y_{s2})^2}\right| = T_i \cdot v_l \quad (1)$$

where $v_l$ is the group velocity of the longitudinal wave. $T_i$ is the difference between the time-of-arrivals of the damage-induced waves reaching the two sensors. By the same token, if multiple sensor pairs are considered, the damage can be located by the intersection of their corresponding hyperbolas. The probability-based damage imaging philosophy is applied to obtain the possibility of damage occurrence at an arbitrary node $i$ $(x, y)$ resulting from a specific sensor pair, which is defined as

$$R_i(x, y) = 1 - \left|\frac{|D_{s1,i,s2}| - D_{d-c}}{D_{s1,i,s2}}\right| \quad (2)$$

where $D_{s1,i,s2}$ is the difference between the distances from a specific node to the two sensors. By synthesizing the damage information from all sensor pairs, the overall possibility of damage occurrence at the node $i$ can be obtained as

$$p_{inner}(x, y) = \sum_{i=1}^{N} R_i(x, y) \quad (3)$$

Finally, a damage image can be further obtained by assessing all the nodes in the inspection area.

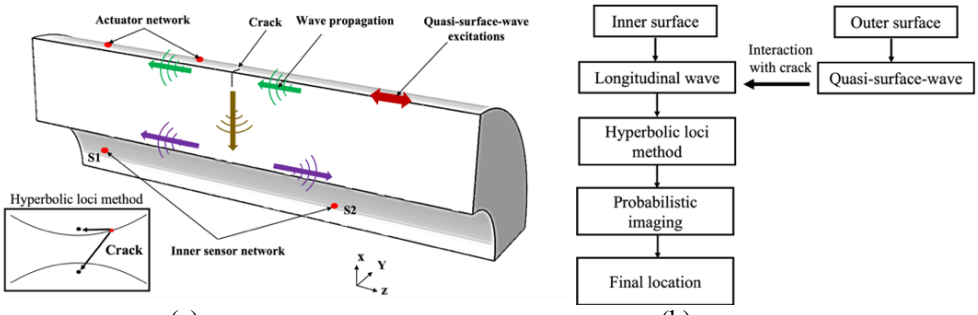


(a) (b)

Figure 4. (a) Sketch of the 3D FE hollow cylinder and damage, (b) Sketch of the localization strategy.

## NUMERICAL VALIDATIONS

### FE Model Description

A 3-D FE model is established in Abaqus/Explicit as sketched in Fig. 5(a). The TWHC model is 300 mm long, with inner and outer radii of 50 mm and 100 mm, respectively. The material parameters used in the simulations are identical to those described and used in Section 2. The excitation is a prescribed displacement in the $z$ direction with a 5-cycle tone burst signal at 300 kHz to mimic a surface-mounted actuator. Similarly, the displacements in the $z$ direction at different sensing locations

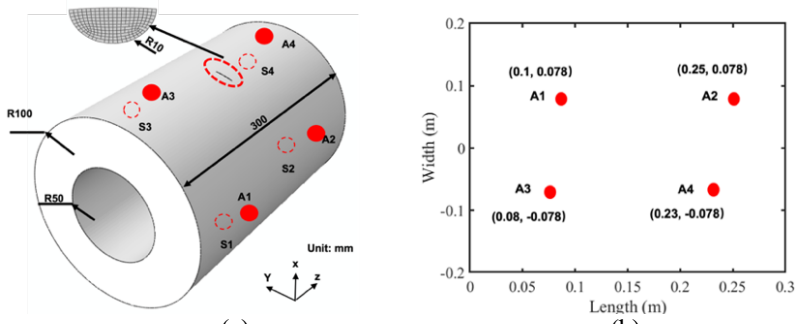


(a) (b)

Figure 5. (a) Sketch of the 3D FE hollow cylinder and damage. A sensor network arrangement over the outer surface: (b) Transducer network configuration.

are extracted as the sensor outputs. A semicircle seam crack with a radius of 10 mm is introduced as a structural damage, which is located at the mid-span of the cylinder over its outer surface. The maximum mesh size used in the FE model is 1 mm, which ensures more than 10 elements per shortest wavelength under consideration. A transducer network configuration, shown in Fig. 5(b), is considered, which is mapped to the outer surface of the cylinder. Transducers on the inner surface are correspondingly installed as illustrated in Fig. 5(a). The transducers on the outer surface are switched on in turn to provide the excitation whilst the remaining transducers on both the inner and outer surfaces serving as sensors.

## Signal Processing and Feature Extraction

Response signals before and after the introduction of the crack are captured which are referred to as the intact and crack status, respectively. Typically, when S1 is used as actuator, the typical response from sensors S3 on the outer surface is shown in Fig. 6(a). The black and red lines represent the intact and crack signals, respectively, which show significant differences. By subtracting the intact signals from the crack signals, the damage-scattering signals can be obtained as indicated by blue lines in both figures. The normalized wavelet coefficients of the damage-scattered signals at different sensor positions are calculated at a center frequency of 300 kHz as shown in Fig. 6(b).

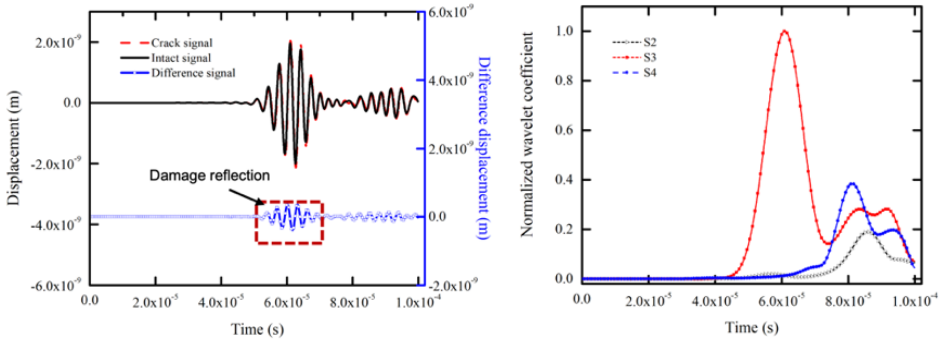


(a) (b)

Figure 6. FE simulated response signals when excitation is applied at S1: (a) time-domain signals at S3; (b) the wavelet coefficients of the damage-scattered signals at the sensors on the inner surface.

## Localization and Sensor Network Comparisons

For the extracted temporal information from the wavelet transform, the damage image is reconstructed with the hyperbolic loci method on the inner surface as shown

in Fig. 7. Specifically, the localization error (the distance between the actual damage center to the identified damage center indicated by the highest Pinner ) is 8 mm.

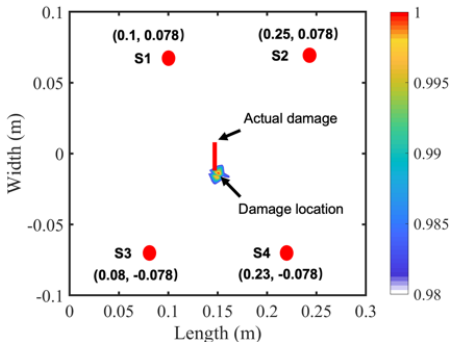


Figure 7. Damage localization results with Configuration A

## EXPERIMENTAL VALIDATION

Experiments are carried out to further validate the proposed localization strategy with an aluminum hollow cylinder of a total length of 500 mm, an inner and outer diameters of 100 mm and 200 mm (see Fig. 8). Eight circular piezoelectric wafer transducers (PZT), 0.5 mm thick and 6 mm in diameter, are bonded onto the outer and inner surfaces of the hollow cylinder with instant glue. The measurement system is shown in Fig. 8. A controller generates a tone burst excitation signal through the KEYSIGHT 33500B Waveform Generator. The signal is amplified by the GA-2500A Gated RF amplifier to drive the PZT actuator. The generated waves are captured by the PZT sensors and recorded by the NI PXIe-5105 data acquisition module. Finally, the response signals are stored and processed by the controller.

Guided by the FE analyzes, four PZTs are mounted on the outer surface of structure and the other four on the inner surface. The 200V 5-cycle Hann-windowed tone burst signal centered at 300 kHz is used. The signals captured by sensors are averaged by 100 measurements to reduce the adverse influence of the measurement noise. A notch, roughly 20 mm long, 1 mm wide and 3 mm deep is fabricated to mimic a structural damage as shown in Fig. 8.

With the extracted temporal information from the damage-scattered signals, damage image is reconstructed for the proposed damage localization strategy in Fig. 9. The identified damage localization is (0.1446 m, 0.00242 m) as indicated by the position of the highest value of $P_{inner}$ and the localization error is 5 mm with respect to the actual damage location at (0.15 m, 0). This further confirms the efficacy of the proposed method.

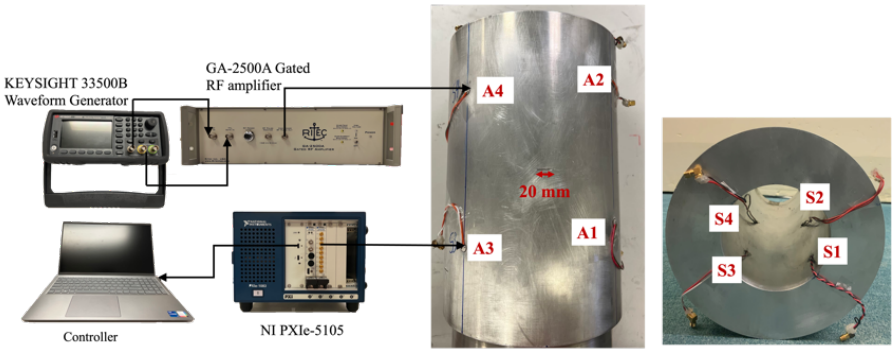


Figure 8. Experimental setup.

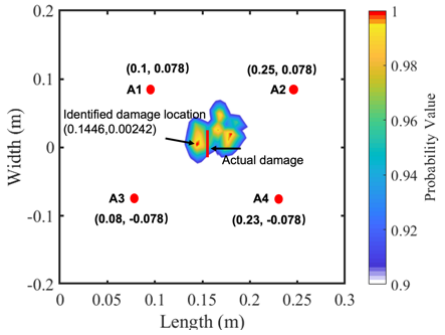

Figure 9. Experimental damage localization results: damage image obtained from the inner strategy.

## CONCLUSIONS

The wave propagation in a TWHC is investigated from both theoretical and numerical perspectives. Based on the acquired understanding, a damage localization strategy is proposed using inner surface sensing. Finite element analyses are first carried out to validate the proposed method and to assess the influence of the transducer network layout. Experimental validations are finally conducted.

Studies reveal that, an outer surface excitation generates dominant quasi-surface waves on the outer surface alongside the shear bulk waves propagating through the wall thickness direction in a TWHC. Reaching the inner surface, the bulk waves are converted into longitudinal waves to propagate along the inner surface rather than quasi-surface waves. Capitalizing on this understanding, damage localization is successfully achieved by using hyperbolic loci method through inner surface sensing, as confirmed by both FE simulations and experiments.

## ACKNOWLEDGMENTS

The work was supported by grants from the Research Grants Council of Hong Kong Special Administrative Region (PolyU 152013/21E), and the Innovation and Technology Commission of the HKSAR Government to the Hong Kong Branch of National Rail Transit Electrification and Automation Engineering Technology Research Center.

## REFERENCES

[1] K. Makino and S. Biwa, "Influence of axle–wheel interface on ultrasonic testing of fatigue cracks in wheelset," *Ultrasonics,* vol. 53, no. 1, pp. 239-248, 2013.

[2] C. R. Farrar and K. Worden, "An introduction to structural health monitoring," *Philosophical Transactions of the Royal Society A: Mathematical, Physical and Engineering Sciences,* vol. 365, no. 1851, pp. 303-315, 2007.

[3] D. C. Gazis, "Three-dimensional investigation of the propagation of waves in hollow circular cylinders. II. numerical results," *The Journal of the Acoustical Society of America,* vol. 31, no. 5, pp. 573-578, 1959.

[4] D. Bancroft, "The velocity of longitudinal waves in cylindrical bars," *Physical Review,* vol. 59, no. 7, p. 588, 1941.

[5] M. Castaings and C. Bacon, "Finite element modeling of torsional wave modes along pipes with absorbing materials," *The Journal of the Acoustical Society of America,* vol. 119, no. 6, pp. 3741-3751, 2006.